Effect of exchange coupling on magnetic property in Sm–Co/α-Fe layered system*

C X Sang(桑成祥)[1,2], G P Zhao(赵国平)[1,2,†], W X Xia(夏卫星)[2,‡], X L Wan(万秀琳)[1], F J Morvan[1], X C Zhang(张溪超)[1], L H Xie(谢林华)[1], J Zhang(张健)[2], J Du(杜娟)[2], A R Yan(闫阿儒)[2], and P Liu(刘平)[2,3]

[1] *College of Physics and Electronic Engineering, Sichuan Normal University, Chengdu* 610066, *China*

[2] *Key Laboratory of Magnetic Materials and Devices, Ningbo Institute of Material Technology and Engineering, Chinese Academy of Sciences, Ningbo* 315201, *China*

[3] *Department of Physics, University of Texas at Arlington, Arlington, TX* 76019, *USA*

(Received 16 September 2015; revised manuscript received 5 November 2015; published online 18 January 2016)

The hysteresis loops as well as the spin distributions of Sm–Co/α-Fe bilayers have been investigated by both three-dimensional (3D) and one-dimensional (1D) micromagnetic calculations, focusing on the effect of the interface exchange coupling under various soft layer thicknesses t^{s}. The exchange coupling coefficient A^{hs} between the hard and soft layers varies from 1.8×10^{-6} erg/cm to 0.45×10^{-6} erg/cm, while the soft layer thickness increases from 2 nm to 10 nm. As the exchange coupling decreases, the squareness of the loop gradually deteriorates, both pinning and coercive fields rise up monotonically, and the nucleation field goes down. On the other hand, an increment of the soft layer thickness leads to a significant drop of the nucleation field, the deterioration of the hysteresis loop squareness, and an increase of the remanence. The simulated loops based on the 3D and 1D methods are consistent with each other and in good agreement with the measured loops for Sm–Co/α-Fe multilayers.

Keywords: hysteresis loops, exchange coupling, micromagnetics, hard/soft bilayers

PACS: 75.70.Cn, 75.40.Mg, 75.30.Gw, 75.50.Ee **DOI:** 10.1088/1674-1056/25/3/037501

1. Introduction

Since an exchange-coupled composite material was proposed by Kneller in 1991,[1] with a hard phase to provide high coercivity and a soft phase to provide high saturation and remanence, the coercivity, structural, and magnetic properties in permanent magnets have always been an important topic in magnetism.[2–4] An energy product paradox was proposed in some literatures, which has been intensively studied in both experimental[5–8] and theoretical[9–15] works by condensed matter physicists. A lot of works have been devoted to the exploration of the largest energy product experimentally reachable. In 1993, Skomski *et al.*[16] proposed that the theoretical energy product $(BH)_{\max}$ of oriented composite magnets could be as large as 120 MG·Oe, which almost doubled that of the best available single-phase permanent magnets.

In order to realize such a giant energy product, many scientists have done a lot of work in the past two decades. A close review shows that the experimental remanence is close to the predicted one, however, the measured coercivity is much smaller.[17–20] Therefore, such an energy product paradox is intrinsically linked to Brown's coercivity paradox, i.e., the measured coercivity is much smaller than that predicted by the available theory. Experimentally, huge progresses have been made recently: an energy product $(BH)_{\max}$ of 60 MG·Oe has been obtained in Nd–Fe–B/Fe–Co multilayers by Cui *et al.*,[5] while a value of 40 MG·Oe has been reached by Sawatzki *et al.* in $SmCo_5$/Fe/$SmCo_5$.[21] It is worth noting that at high temperature, the magnetic properties of Nd–Fe–B are inferior to those of Sm–Co due to a lower Curie temperature (about 400 °C against 800 °C), which can occasionally make Sm–Co a better choice compared to Nd–Fe–B.

In the pursuit of the highest energy product reachable, a new structure has been discovered and investigated: the inclusion of an interface layer within bilayers. Choi *et al.*[22] found that the maximum energy product of Sm–Co/α-Fe bilayers can be improved by 50% with an intermixed interface layer, and reach a value of 15 MG·Oe. Zhang *et al.*[23–25] discovered that by inserting thin non-magnetic spacer layers like Cu in $SmCo_5$/Fe, increased coercivity and pinning fields can be realized. As a result, $(BH)_{\max}$ jumps from 9 MG·Oe to 32 MG·Oe with a coercivity of 7.24 kOe. The single-phase behavior and the irreversible rotation in the demagnetization pro-

*Project supported by the National Natural Science Foundation of China (Grant Nos. 11074179 and 10747007), the National Basic Research Program of China (Grant No. 2014CB643702), the Zhejiang Provincial Natural Science Foundation of China (Grant No. LY14E010006), the Construction Plan for Scientific Research Innovation Teams of Universities in Sichuan Province, China (Grant No. 12TD008), the Scientific Research Foundation for the Returned Overseas Chinese Scholars of the Education Ministry, China, and the Program for Key Science and Technology Innovation Team of Zhejiang Province, China (Grant No. 2013TD08).

†Corresponding author. E-mail: zhaogp@uestc.edu.cn

‡Corresponding author. E-mail: xiawxing@nimte.ac.cn

© 2016 Chinese Physical Society and IOP Publishing Ltd

cess indicates a strong exchange coupling between the Sm(Co, Cu)$_5$ and Fe layers. Moreover, Liu *et al.*[26] discovered that the Fe/Co mixture behavior enhances the interface exchange-coupling and improves the remanence as well as the coercivity of the composite magnet.

In a word, the interface exchange coupling is important in realizing good magnetic properties in Sm–Co/α-Fe layered systems, which, however, have seldom been investigated systematically in theory. In this paper, three-dimensional (3D) micromagnetic simulations and analytical calculations are performed for Sm–Co/α-Fe bilayers, which are then compared to our experimental results. This work focuses on the influence of the exchange coupling and the soft phase thickness on the coercivity and nucleation fields of the system.

2. 3D simulation and 1D calculation model

Our calculation is based on an exchange-coupled bilayer (see Fig. 1). An *o-xyz* coordinate system is constructed with the origin located at the center of the interface. The magnetocrystalline axes of both layers and the applied field are assumed to be in the *y* direction, as shown in Fig. 1.

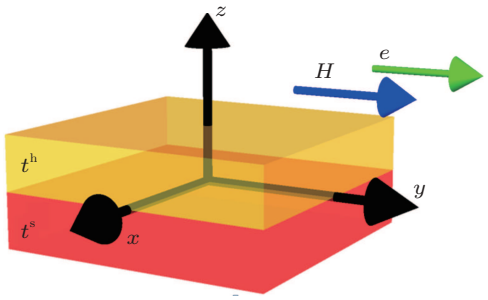


Fig. 1. (color online) Basic scheme of the investigated hard/soft bilayers in the three-dimensional micromagnetic model.

The 3D micromagnetic calculation of the software OOMMF is based on the Landau–Lishitz–Gilbert dynamic equation[27]

$$\frac{\mathrm{d}\boldsymbol{M}}{\mathrm{d}t} = -\frac{\gamma}{1+\alpha^2}\boldsymbol{M}\times\boldsymbol{H}_{\mathrm{eff}} - \frac{\alpha\gamma}{(1+\alpha^2)M_{\mathrm{s}}}\boldsymbol{M}\times(\boldsymbol{M}\times\boldsymbol{H}_{\mathrm{eff}}), \quad (1)$$

where $\boldsymbol{M}$ is the magnetization, $\boldsymbol{H}_{\mathrm{eff}}$ is the effective field, γ is the gyromagnetic ratio, and α is the damping coefficient. Since the damping coefficient in our case has little influence on the results obtained, α is set at 0.5 to make a good balance between the calculation precision and the computation speed. The effective field is defined as

$$\boldsymbol{H}_{\mathrm{eff}} = -\mu_0^{-1}\frac{\partial E}{\partial \boldsymbol{M}}, \quad (2)$$

where the average energy density E is a function of $\boldsymbol{M}$ specified by Brown's equations,[28] including the exchange, anisotropy, applied field (Zeeman), and magnetostatic (demagnetization) terms.

In the 3D simulations, the system is set as a tetragonal box of sizes 300 nm×300 nm×t. The variable t is the thickness of the layers, namely, $t = t^{\mathrm{h}} + t^{\mathrm{s}}$, as shown in Fig. 1. The subscripts s and h stand for the soft and hard layers, respectively. The thickness of the hard layer t^{h} is set as 10 nm, while the thickness of the soft layer $t^{\mathrm{s}} = 2$ nm, 6 nm, and 10 nm. The magnetic structure within these thin layers is discretized into 3 nm×3 nm×1 nm cells, which has been optimized to achieve a balance between calculation accuracy and computation time.

In this paper, Sm–Co is chosen as the hard layer, while α-Fe is the soft layer. The material parameters used in the simulation are: $M^{\mathrm{s}} = 1.71\times10^3$ emu/cc, $M^{\mathrm{h}} = 5.5\times10^2$ emu/cc, $K^{\mathrm{s}} = 4.6\times10^5$ erg/cc, $K^{\mathrm{h}} = 5\times10^7$ erg/cc, $A^{\mathrm{s}} = 2.5\times10^{-6}$ erg/cm, and $A^{\mathrm{h}} = 1.2\times10^{-6}$ erg/cm, which are adopted from Refs. [15], [29], and [30]. Here, A, K, and M denote the exchange energy constant, the anisotropy constant, and the spontaneous magnetization, respectively. Only the exchange interaction between the neighboring region pair is taken into account and the free boundary conditions are chosen. The interface coupling is difficult to describe precisely, as it depends not only on the bulk crystalline structures of the hard and soft layers, but also on the strength of the interface exchange coupling. The exchange energy constant between the soft and hard layers A^{hs} is set as 1.8×10^{-6} erg/cm when Sm–Co/α-Fe is in full coupling, while it is taken as 0.9×10^{-6} erg/cm and 0.45×10^{-6} erg/cm for low coupling.

The analytical calculation is carried out supposing all layers extending to infinity, which is referred to as the 1D method. The magnetization can be calculated as a function of z, given that the magnetization is uniform within the layer plane (xy plane). The energy density per area in the film plane is[15,29,31,32]

$$\begin{aligned} v = &\int_0^{t^{\mathrm{h}}}\left[A^{\mathrm{h}}\left(\frac{\mathrm{d}\theta}{\mathrm{d}z}\right)^2 + K^{\mathrm{h}}\sin^2\theta - \mu_0 H M_{\mathrm{s}}^{\mathrm{h}}\cos\theta\right]\mathrm{d}z \\ &+ \int_{-t^{\mathrm{s}}}^{0}\left[A^{\mathrm{s}}\left(\frac{\mathrm{d}\theta}{\mathrm{d}z}\right)^2 + K^{\mathrm{s}}\sin^2\theta - \mu_0 H M_{\mathrm{s}}^{\mathrm{s}}\cos\theta\right]\mathrm{d}z \\ &- \frac{j^{\mathrm{i}}}{a^2}(m^{\mathrm{s}}m^{\mathrm{h}} - 1), \end{aligned} \quad (3)$$

where a is the distance between the adjacent atomic planes near the interface, θ is the angle between the magnetization and the applied field, and m and j^{i} are the magnetization unit vector at the interface and the interlayer coupling constant, respectively. The three terms inside the bracket of the above formula are the exchange, anisotropy, and Zeeman energies, respectively, while the last term is the interface exchange coupling energy.

By applying the variational method to the interface exchange coupling energy with suitable boundary conditions, we

obtain

$$\left.\frac{\mathrm{d}\theta}{\mathrm{d}z}\right|_{z=-t^{\mathrm{s}}} = 0, \quad \left.\frac{\mathrm{d}\theta}{\mathrm{d}z}\right|_{z=t^{\mathrm{h}}} = 0, \tag{4}$$

$$A^{\mathrm{h}}\left.\frac{\mathrm{d}\theta}{\mathrm{d}z}\right|_{z=0^{+}} = A^{\mathrm{s}}\left.\frac{\mathrm{d}\theta}{\mathrm{d}z}\right|_{z=0^{-}} = \frac{j^{\mathrm{i}}}{2a^2}\sin(\theta_{0^{+}} - \theta_{0^{-}}), \tag{5}$$

where $j^{\mathrm{i}} = 2a^2A^{\mathrm{hs}}/c$, with c the distance between the atomic planes of the soft and hard layers. Sm–Co has a tetragonal structure with lattice constants $a = 0.49$ nm and $c = 0.41$ nm,[32] while α-Fe is in a structure with a lattice constant of 0.29 nm. The θ_0^+ and θ_0^- are respectively the angles at $z = 0^+$ and $z = 0^-$ of the hard/soft interface. It should be noted that $\theta_0^+ = \theta_0^-$ when $j^{\mathrm{i}} = \infty$.

In particular, at the nucleation state, the deviation of the magnetization from the applied field direction is small. Thus, the nucleation problem can be solved by an appropriate ansatz or series expansion[14]

$$\frac{\pi t^{\mathrm{s}}}{\Delta^{\mathrm{s}}} = \frac{\tan^{-1}\left(\dfrac{\sqrt{A^{\mathrm{h}}K^{\mathrm{h}}(h_{\mathrm{N}}^{\mathrm{h}}+1)}}{\sqrt{A^{\mathrm{s}}K^{\mathrm{s}}(-h_{\mathrm{N}}^{\mathrm{s}}-1)}}\right)}{\left(1+\dfrac{2a^2}{j^{\mathrm{i}}}\sqrt{A^{\mathrm{h}}K^{\mathrm{h}}(h_{\mathrm{N}}^{\mathrm{h}}+1)}\right)\sqrt{-h_{\mathrm{N}}^{\mathrm{h}}-1}}, \tag{6}$$

where $h = H/H_K$ represents the reduced applied field with $H_K = 2K/M_{\mathrm{s}}$ the anisotropy field, and $\Delta = \pi(A/K)^{1/2}$ is the Bloch wall width.

3. Calculated hysteresis loops

Figure 2(a) shows the calculated hysteresis loops of Sm–Co/α-Fe bilayers for various interface exchange couplings by 3D simulations, where the thicknesses of the hard and soft layers are set as $t^{\mathrm{h}} = 10$ nm and $t^{\mathrm{s}} = 2$ nm. It can be seen that the shapes of the hysteresis loops are not sensitive to the exchange coupling between the hard and soft layers, the loops demonstrate a typical exchange-spring magnetic phase for all three values of exchange coupling.[15,29] As the exchange coupling decreases, the hysteresis loop becomes more slanted, accompanied by a slight decrease of the nucleation field. As A^{hs} decreases, both pinning and coercive fields increase gradually. On the other hand, the nucleation field decreases, leading to the deterioration of the squareness of the loop. As shown in Fig. 2(a) and summarized in Table 1, the pinning field for $A^{\mathrm{hs}} = 4.5 \times 10^{-7}$ erg/cm is about 20% larger than that for $A^{\mathrm{hs}} = 1.8 \times 10^{-6}$ erg/cm. Figure 2(b) shows the calculated hysteresis loops of Sm–Co/α-Fe bilayers for various A^{hs} based on the 1D calculation, where $t^{\mathrm{h}} = 10$ nm and $t^{\mathrm{s}} = 2$ nm. Since for arbitrary applied fields, the angular distribution of θ can be obtained by Eq. (3), and averaging $M_{\mathrm{s}}\cos\theta$ from $z = -t^{\mathrm{s}}$ to t^{h}, one can obtain the major hysteresis loop for a given hard/soft bilayer. The 1D calculations yield similar loops compared to those obtained by the 3D simulations, justifying our models. As A^{hs} decreases, both pinning and coercive fields increase gradually whereas the nucleation field decreases, leading to the deterioration of the squareness of the loop. In the meantime, the nucleation field departs from the coercivity and the gap between the two fields enlarges. For all values of A^{hs}, the pinning field and the coercivity are equal to each other, signifying a coercivity mechanism of pinning.

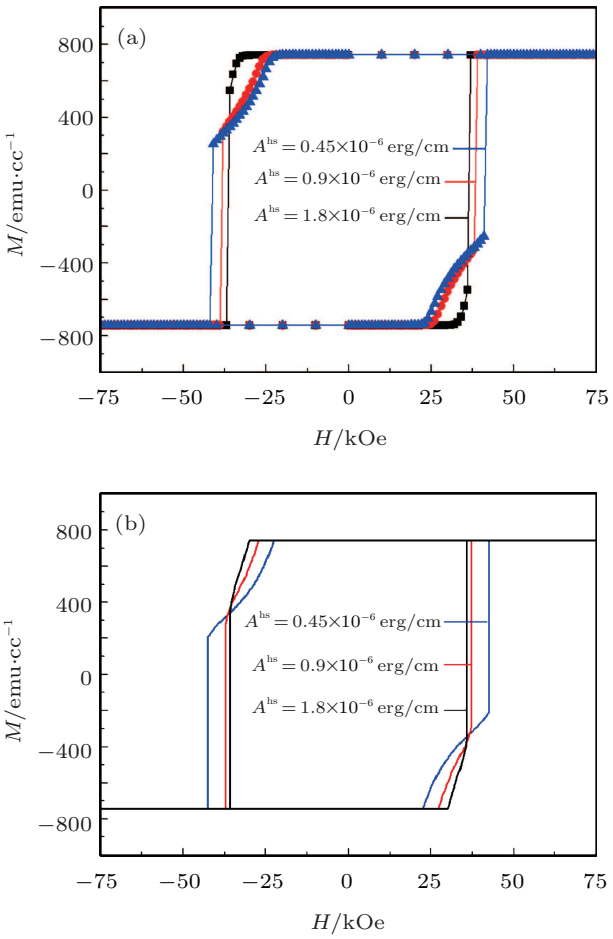


Fig. 2. (color online) Macroscopic hysteresis loops of Sm–Co(10 nm)/α-Fe(2 nm) bilayers obtained by (a) 3D simulations and (b) analytical calculations.

When Sm–Co/α-Fe has an exchange coupling of $A^{\mathrm{hs}} = 1.8 \times 10^{-6}$ erg/cm, the shape of the hysteresis loop is essentially a rectangle according to the 3D simulations, where the nucleation and pinning fields are close to each other. When A^{hs} decreases from 1.8×10^{-6} erg/cm to 4.5×10^{-7} erg/cm, the gap between nucleation and pinning fields rises from 3.5 kOe to 21 kOe. On the other hand, there is an obvious nucleation point at the applied field of -29.6 kOe for $A^{\mathrm{hs}} = 1.8 \times 10^{-6}$ erg/cm according to the 1D calculation, which is quite different from the corresponding pinning point at $H = -35.8$ kOe. This gap between the nucleation and pinning fields rises to 20 kOe as A^{hs} decreases to 4.5×10^{-7} erg/cm.

Table 1. Calculated magnetic properties of Sm–Co/α-Fe based on the OOMMF software and 1D calculation, where $t^{\rm h} = 10$ nm.

$t^{\rm s}$/nm	$A^{\rm hs}/10^{-6}$erg·cm^{-1}	Method	$H_{\rm N}$/kOe	$H_{\rm c}$/kOe	$H_{\rm p}$/kOe	$M_{\rm r}$/emu·cc^{-1}
2	1.8	1D	30.0	35.8	35.8	743.49
		3D	32.69	36.15	36.15	742.46
	0.9	1D	27.0	37.2	37.2	743.49
		3D	24.49	38.50	38.50	742.46
	0.45	1D	22.5	42.5	42.5	743.49
		3D	20.01	41.27	41.27	742.46
6	1.8	1D	8.5	15.6	19	985.37
		3D	6.65	15.01	15.37	982.99
	0.9	1D	7.7	15.4	21.5	985.37
		3D	5.75	15.05	21.97	982.99
	0.45	1D	6.7	13.95	28.8	985.37
		3D	4.91	14.21	27.19	982.99
10	1.8	3D	2.96	8.30	20.51	1043.68
	0.9	3D	2.93	6.82	12.60	1043.68

As shown in the previous studies,[13–15,29] the hysteresis loop and the coercivity mechanism are sensitive to the soft layer thickness. Zhao *et al*. found that as the soft layer thickness increases, the coercivity mechanism changes from nucleation to pinning when the hard layer is large enough. Besides, Asti *et al*. found that the magnetic phase diagram changes from rigid composite magnet to exchange-spring and finally to decoupled magnet with the increase of the soft layer thickness. Therefore, the hysteresis loops are calculated for various $A^{\rm hs}$ with $t^{\rm s} = 6$ nm, as shown in Fig. 3. Similar to the case with $t^{\rm s} = 2$ nm, both pinning and coercive fields go up whereas the nucleation field goes down as $A^{\rm hs}$ decreases, leading to the deterioration of the squareness of the loop. In contrast with Fig. 2, where the squareness of the loops is quite good, the loops in Fig. 3 demonstrate much worse squareness, in particular for $A^{\rm hs} = 4.5 \times 10^{-7}$ erg/cm. Indeed, at this point, the pinning field is about 5.5 times the corresponding nucleation field according to the 3D simulations, demonstrating a typical decoupled magnetic phase.[15,29] The calculated maximum energy products based on Fig. 3(a) are 38 MG·Oe, 37 MG·Oe, and 35 MG·Oe for $A^{\rm hs} = 1.8 \times 10^{-6}$ erg/cm, $A^{\rm hs} = 0.9 \times 10^{-6}$ erg/cm, and $A^{\rm hs} = 0.45 \times 10^{-6}$ erg/cm, respectively.

Figure 4 shows the calculated spin configurations in the y–z plane for Sm–Co(10 nm)/α-Fe(6 nm) bilayers with $A^{\rm hs} = 1.8 \times 10^{-6}$ erg/cm. The results in Figs. 4(a)–4(e) correspond to the points A–E in the hysteresis loop shown in Fig. 3(a), respectively. The small and large arrows denote the magnetic moments within the Sm–Co and α-Fe layers, respectively, and are proportional to their magnetization. At $H = 0$ kOe (Fig. 4(a), point A), all the magnetic moments in the system orient parallel to the y axis. At $H = -7.0$ kOe (Fig. 4(b), point B), the magnetization begins to deviate from the previous saturation state incoherently. At $H = -12.0$ kOe (Fig. 4(c), point C), one can find that the magnetic moments in the α-Fe layer far away from the interface have rotated 90°, while those near the interface are pinned by the exchange coupling with the Sm–Co layer. When the applied field decreases to -15.0 kOe (Fig. 4(d), point D), most magnetic moments in the α-Fe layer have reversed, while the magnetic moments in the Sm–Co layer far away from the interface have hardly rotated due to the large crystalline anisotropy, forming a 180° domain wall at the interface. At $H = -16$ kOe (Fig. 4(e), point E), the magnetic moments in both hard and soft phases have reversed completely.

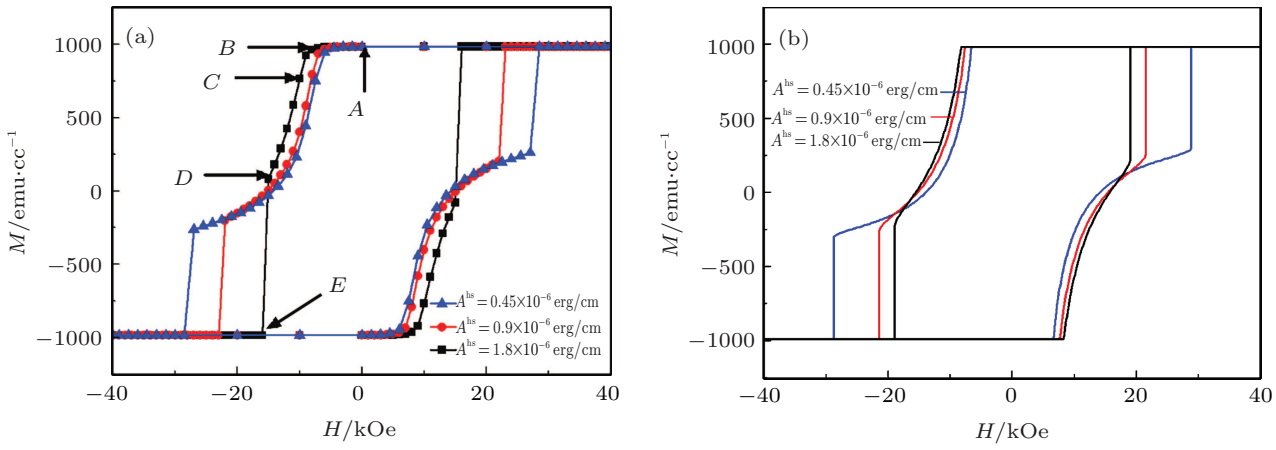


Fig. 3. (color online) Macroscopic hysteresis loops of Sm–Co(10 nm)/α-Fe(6 nm) bilayers obtained by (a) 3D simulations and (b) analytical calculations.

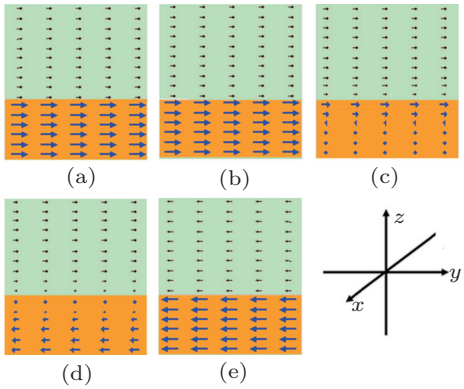


Fig. 4. (color online) 2D evolution of the magnetization calculated by OOMMF for Sm–Co(10 nm)/α-Fe(6 nm) with exchange coupling $A^{\rm hs} = 1.8 \times 10^{-6}$ erg/cm: (a) $H = 0$ kOe, magnetization saturation, (b) $H = -7.0$ kOe, near nucleation field, (c) $H = -12.0$ kOe, between the nucleation and coercive fields, (d) $H = -15.0$ kOe, the coercive field, (e) $H = -16.0$ kOe, the pinning point.

Experimentally, the interface of the hard/soft layers has been intensively modified to obtain the best performance for the exchange spring film. A spacing layer Ta was inserted between $Nd_2Fe_{14}B$ and FeCo layers to adjust the exchange coupling and magnetostatic interaction to obtain the largest $(BH)_{\rm max}$ in NdFeB-based nanocompiste films.[5] For the SmCo/Fe system, a diffusion layer was reported to be effective for getting a larger nucleation field and hence $(BH)_{\rm max}$.[6] A Cu layer was used in multilayer films Cr(50 nm)/[$SmCo_6$(9 nm)/Cu(x nm)/Fe(5 nm)/Cu(x nm)]$_6$ /Cr(100 nm)/SiO_2 (x = 0–0.75) and a high $(BH)_{\rm max}$ of 32 MG·Oe was obtained by some of us.[23–25] Although the Cu layer promotes the crystallization of the SmCo phase to form a uniform multilayer, the Cu layer with different thickness is considered to adjust the exchange coupling as well. In the case of the SmCo layer directly contacting the Fe layer, the exchange coupling is strong. With the Cu thickness increased, the soft and hard phases are separated by the Cu layer, which results in a decrease of the exchange coupling. Figure 5 demonstrates the measured hysteresis loops of two SmCo/Cu/Fe multilayers at 10 K and the calculated loops based on OOMMF. It can be observed that the trend of the experimental loops (with the Cu layer thickness increasing from 0 to 0.75 nm) is consistent with that of the calculated loops (with $A^{\rm hs}$ decreasing from 1.8×10^{-6} erg/cm to 0.9×10^{-6} erg/cm). The smoothness and two-stage feature in the calculated loops are due to the ideal material parameters adopted in the calculation, while in experiment, the more complicated polycrystalline structure, dispersion in the composition, and defects exist, therefore the intrinsic property of the material is affected. Nevertheless, our calculation data show qualitative agreement with the experiment one.

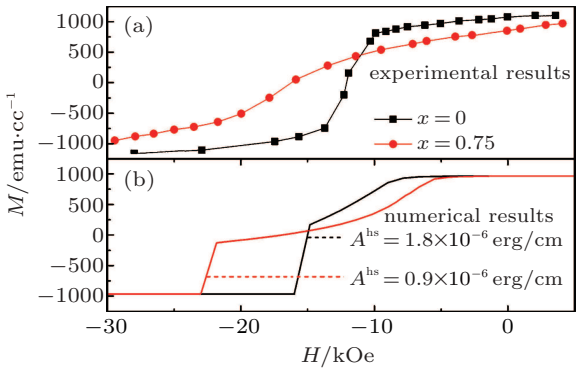


Fig. 5. (color online) Comparison of calculated hysteresis loops with experimental loops for Cr(50 nm)/[$SmCo_6$(9 nm)/Cu(x nm)/Fe(5 nm)/Cu(x nm)]$_6$ /Cr(100 nm)/a-SiO_2 (x = 0–0.75). (a) The black squares are for the sample with $x = 0$ annealed at 500 °C measured at 10 K while the red circles are for the sample with $x = 0.75$ annealed at 500 °C measured at 10 K. (b) The black lines are for $t^{\rm h} = 9$ nm, $t^{\rm s} = 5$ nm, and $A^{\rm hs} = 1.8 \times 10^{-6}$ erg/cm; while the red lines are for $t^{\rm h} = 9$ nm, $t^{\rm s} = 5$ nm, and $A^{\rm hs} = 0.9 \times 10^{-6}$ erg/cm using OOMMF.

4. Angular distribution of magnetization

Figure 6 demonstrates the angular distributions of magnetization in the $+z$ direction for Sm–Co (10 nm)/α-Fe (2 nm) bilayers with identical exchange coupling $A^{\rm hs} = 0.45 \times 10^{-6}$ erg/cm based on 1D and 3D models. In the analytical model, the angular distributions of magnetization in the z direction can be obtained by minimizing the energy density expressed in Eq. (3), which is coherent in the x–y plane. With the 3D calculation, the angular distributions are obtained by averaging the component of all the magnetic moments in the applied field direction with a certain z.

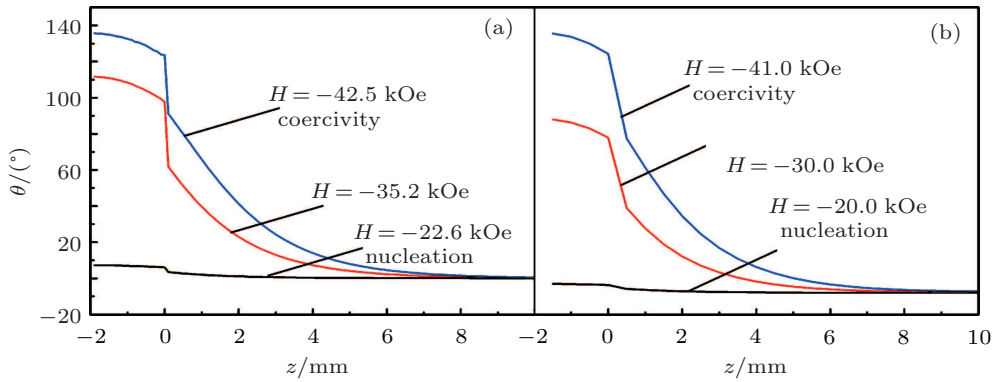


Fig. 6. (color online) Calculated spatial distributions of magnetization direction for Sm–Co(10 nm)/Fe(2 nm) bilayers based on (a) analytical calculations and (b) 3D simulations with exchange coupling $A^{\rm hs} = 0.45 \times 10^{-6}$ erg/cm.

As shown in Fig. 6(a), a small deviation of the magnetization from the previous saturation state occurs at $H = -22.6$ kOe, which is called nucleation according to Brown. Under this field, a 7.11° infant domain wall has been formed with $\theta^{\rm h} = 0°$, $\theta^{0+} = 2.98°$, $\theta^{0-} = 6.26°$, and $\theta^{\rm s} = 7.11°$. The domain wall grows fast as the applied field reduces. When the applied field reaches $H = -35.2$ kOe, a 110° domain wall forms. Further decrease of the applied field leads to a faster growth of the domain wall. At the coercive point, it reaches its maximum with a value of 136° when the applied field drops to -42.5 kOe. Additional decrease of the applied field will result in the magnetic reversal of the whole bilayer system. In Fig. 6, the 3D simulation and the 1D calculation show the same results.

5. Critical fields

From the above discussion, one can find that a large nucleation field is essential to keep the squareness of the corresponding hysteresis loop. In this section, the dependence of this critical field on the exchange interaction and the soft layer thickness is discussed. In nanocomposite films, the hard phase offers a high anisotropy to produce the high coercivity, but this effect strongly depends on its thickness. If $t^{\rm h}$ is smaller than the corresponding Bloch wall width,[14,30] which is about 4.9 nm for Sm–Co, its magnetization will be easily reversed by the soft phase through the exchange interaction. While if $t^{\rm h}$ is large enough, the magnetic properties will not depend on it.[33] Therefore, in the calculation below, the thickness of the hard phase is set to 10 nm, which is larger than the Bloch wall width.

Figure 7 and Table 1 demonstrate the calculated nucleation fields for various exchange interactions and soft film thicknesses based on Eq. (6). For comparison, the hysteresis loops in the case of $t^{\rm s} = 2$ nm are calculated using 3D OOMMF and the 1D method, and the nucleation fields are obtained from the loops. One can find that the three methods yield roughly the same nucleation fields. When $A^{\rm hs}$ approaches 0, $H_{\rm N}$ comes close to 0.53 kOe, i.e., the nucleation field of the single α-Fe phase, and at this point, the system degenerates into a typical decoupled magnetic system. With increased exchange interactions, $H_{\rm N}$ increases and approaches some constant value for large $A^{\rm hs}$, which refers to the case of an infinite exchange coupling $A^{\rm hs} = \infty$. In the case of a constant exchange interaction, $H_{\rm N}$ increases when the soft layer thickness decreases.

The nucleation field as a function of the thickness of the α-Fe layer under various exchange interactions $A^{\rm hs}$ is shown in Fig. 8. The value of 180 kOe is found when $d_{\rm Fe} = 0$, which is close to the anisotropy field of Sm–Co (181.8 kOe). The nucleation field decreases when $d_{\rm Fe}$ increases, the strong decline in the region from $d_{\rm Fe} = 0$ nm to ~4 nm is in accordance with the theoretical predictions of Leineweber,[32] Zhao,[34,35] and other numerical simulations.[29,36] From $d_{\rm Fe} = 0$ nm to 10 nm, the nucleation fields with a strong exchange coupling are always larger than those with a weak coupling. A large gap exists between $d_{\rm Fe} \approx 0.5$ nm and $d_{\rm Fe} \approx 5.0$ nm. In the case of $A^{\rm hs} = 1.8 \times 10^{-6}$ erg/cm, the nucleation fields and coercivities obtained by the 1D method and 3D OOMMF are shown in Fig. 8 as well. When $t^{\rm s}$ is smaller than 1.0 nm, the loops are rectangular and the nucleation fields are equal to the coercivities or pinning fields; this thickness is denoted as the first critical thickness,[34] which can be estimated by $t_{\rm crit1} = \pi(A^{\rm s}/2K^{\rm h})^{1/2}$.[1] Using analytical micromagnetics, Zhao *et al.* found that the first critical thickness is inversely proportional to the square root of the magnetocrystalline anisotropy constant of the hard phase, which is consistent with the above formula. With $d_{\rm Fe}$ larger than 1.0 nm, the nucleation and coercive fields deviate and the hysteresis loop gradually loses its squareness.[34,35]

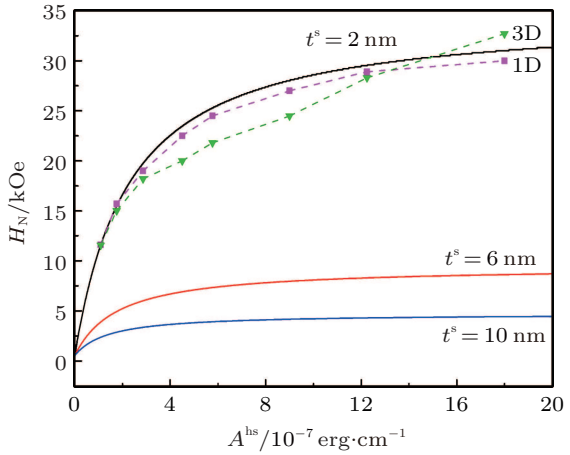


Fig. 7. (color online) Calculated nucleation field as a function of the exchange coupling $A^{\rm hs}$. The solid lines are obtained with Eq. (6). The dashes are calculated with 1D and 3D models.

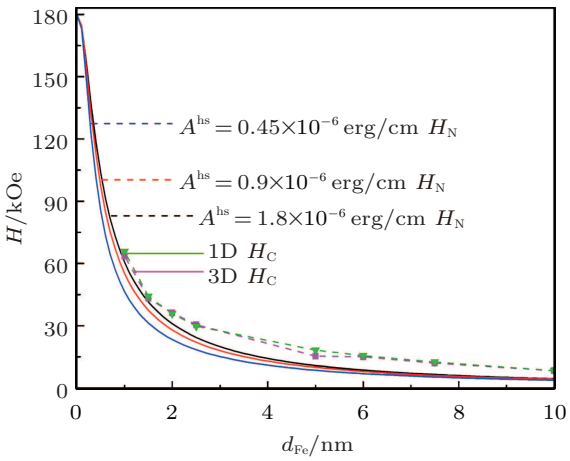


Fig. 8. (color online) Calculated nucleation and coercive fields as a function of the soft layer thickness $t^{\rm s}$. The solid lines are obtained with Eq. (6). The dashes are calculated with 1D and 3D models.

6. Conclusion

The effects of the exchange coupling on magnetic properties were investigated for Sm–Co/α-Fe bilayers using a 3D micromagnetic software OOMMF and a 1D analytical model. A reduced exchange coupling results in lower nucleation fields and higher coercivities. Both methods show agreeable results with the experimental multilayer data. On the other hand, when the soft layer thickness increases, both pinning field and remanence increase whereas the nucleation and coercive fields decrease, leading to the deterioration of the squareness of the loops. The calculated results can partially explain Brown's coercivity paradox in hard/soft composite materials. A strong exchange coupling is essential to keep the squareness, therefore a large energy product.

References

[1] Kneller E F and Hawig R 1991 *IEEE Trans. Magn.* **27** 3588
[2] Tang J, Ma B, Zhang Z Z and Jin Q Y 2010 *Chin. Phys. Lett.* **27** 077502
[3] Zhang W, Zhai Y, Lu M, You B, Zhai H R and Caroline G M 2015 *Chin. Phys. B* **24** 047502
[4] Luo Z Y, Tang J, Ma B, Zhang Z Z, Jin Q Y and Wang J P 2012 *Chin. Phys. Lett.* **29** 127501
[5] Cui W B, Takahashi Y K and Hono K 2012 *Adv. Mater.* **24** 6530
[6] Jiang J S, Pearson J E, Liu Z Y, Kabius B, Trasobares S, Miller D J, Bader S D, Lee D R, Haskel D and Srajer G and Liu J P 2004 *Appl. Phys. Lett.* **85** 5293
[7] Yuan F T, Hsiao S N, Liao W M, Chen S K and Yao Y D 2006 *J. Appl. Phys.* **99** 08E915
[8] Tang J, Yang L R, Wang X J, Zhang L, Wei C F, Chen B W and Mei Y 2012 *Acta Phys. Sin.* **61** 240701 (in Chinese)
[9] Belemuk A M and Chui S T 2011 *J. Appl. Phys.* **110** 073918
[10] Xia J, Zhao G P, Zhang H W, Cheng Z H, Feng Y P, Ding J and Yang H T 2012 *J. Appl. Phys.* **112** 013918
[11] Wong D W, Sekhar M C, Gan W L, Purnama I and Lew W S 2015 *J. Appl. Phys.* **117** 17A747
[12] Belemuk A M and Chui S T 2011 *J. Appl. Phys.* **109** 093909
[13] Zhao G P, Zhao M G, Lim H S, Feng Y P and Ong C K 2005 *Appl. Phys. Lett.* **87** 162513
[14] Zhao G P and Wang X L 2006 *Phys. Rev. B* **74** 012409
[15] Asti G, Ghidini M, Pellicelli R, Pernechele C, Solzi M, Albertini F, Casoli F, Fabbrici S and Pareti L 2006 *Phys. Rev. B* **73** 094406
[16] Skomki R and Coey J M D 1993 *Phys. Rev. B* **48** 15812
[17] Zhang T L, Liu H Y, Liu J H and Jiang C B 2015 *Appl. Phys. Lett.* **106** 162403
[18] Fullerton E E, Jiang J S and Bader S D 1999 *J. Magn. Magn. Mater.* **200** 392
[19] Sellmyer D J 2002 *Nature* **420** 374
[20] Liu W, Zhang Z D, Liu J P, Chen L J, He L L, Liu Y, Sun X K and Sellmyer D J 2002 *Adv. Mater.* **14** 1832
[21] Sawatzki S, Heller R and Mickel C 2011 *J. Appl. Phys.* **109** 123922
[22] Choi Y, Jiang J S, Pearson J E, Bader S D, Kavich J J, Freeland J W and Liu J P 2007 *Appl. Phys. Lett.* **91** 072509
[23] Zhang J, Li Y X, Wang F, Shen B G and Sun J R 2010 *J. Appl. Phys.* **107** 043911
[24] Zhang J, Wang F, Zhang Y, Song J Z, Zhang Y, Shen B G and Sun J R 2012 *J. Nanosci. Nanotechno.* **12** 1109
[25] Zhang J, Takahashi Y K, Gopalan R and Hono K 2005 *Appl. Phys. Lett.* **86** 122509
[26] Liu X B and Altounian Z 2012 *J. Appl. Phys.* **111** 07B526
[27] Donahue M J and Porter D G 1999 *OOMMF User's Guide*, version 1.0. NISTIR 6376, NIST, Gaithersburg, MD
[28] Brown J W F 1945 *Rev. Mod. Phys.* **17** 15
[29] Asti G, Ghidini M and Neri F M 2004 *Phys. Rev. B* **69** 174401
[30] Zhao G P, Deng Y, Zhang H W, Chen L, Feng Y P and Bo N 2010 *J. Appl. Phys.* **108** 093928
[31] Leineweber T and Kronmüller H 1997 *Phys. Status Solidi B* **201** 291
[32] Leineweber T and Kronmüller H 1997 *J. Magn. Magn. Mater.* **176** 145
[33] Zhao G P, Deng Y, Zhang H W, Cheng Z H and Ding J 2011 *J. Appl. Phys.* **109** 07D340
[34] Zhao G P, Morvan F J and Wan X L 2014 *Rev. Nanosci. Nanotechno.* **3** 227
[35] Zhao G P, Zhang X F and Morvan F J 2015 *Rev. Nanosci. Nanotechno.* **4** 1
[36] Fullerton E E, Jiang J S, Grimsaitch M, Sowers C H and Bader S D 1998 *Phys. Rev. B* **58** 12193